

RESEARCH ARTICLE

Deregulation of the imprinted DLK1-DIO3 locus ncRNAs is associated with replicative senescence of human adipose-derived stem cells

Silvia García-López^{1,2^{¶a}}, Carmen Albo-Castellanos^{2^{¶b}}, Rocio G. Urduñigo³, Susana Cañón^{1,2}, Fátima Sánchez-Cabo⁴, Alberto Martínez-Serrano⁵, Mario F. Fraga³, Antonio Bernad^{1,2,*}



1 Department of Immunology and Oncology, Centro Nacional de Biotecnología (CNB-CSIC), Campus de Cantoblanco, Madrid, Spain, **2** Department of Cardiovascular Development and Repair, Centro Nacional de Investigaciones Carlos III (CNIC), Madrid, Spain, **3** Cancer Epigenetics Laboratory, Institute of Oncology of Asturias (IUOPA), Hospital Universitaria Central de Asturias (HUCA) and Nanomaterials and Nanotechnology Research Center (CINN-CSIC), Universidad de Oviedo (UO), Asturias, Spain, **4** Bioinformatics Unit, Centro Nacional de Investigaciones Cardiovasculares Carlos III (CNIC), Madrid, Spain, **5** Molecular Biology Department (UAM) and Molecular Neuropathology Department, Center of Molecular Biology Severo Ochoa-CSIC, Universidad Autónoma de Madrid, Campus Cantoblanco, Madrid, Spain

^{¶a} Current address: Molecular Biology Department (UAM) and Molecular Neuropathology Department, Center of Molecular Biology Severo Ochoa-CSIC, Universidad Autónoma de Madrid, Campus Cantoblanco, Madrid, Spain

^{¶b} Current address: VIVEbioTECH. Gipuzkoako Zientzia eta Teknologia Parkea, Donostia, Gipuzkoa, Spain
* abernad@cnb.csic.es

OPEN ACCESS

Citation: García-López S, Albo-Castellanos C, Urduñigo RG, Cañón S, Sánchez-Cabo F, Martínez-Serrano A, et al. (2018) Deregulation of the imprinted DLK1-DIO3 locus ncRNAs is associated with replicative senescence of human adipose-derived stem cells. PLoS ONE 13(11): e0206534. <https://doi.org/10.1371/journal.pone.0206534>

Editor: Klaus Roemer, Universitat des Saarlandes, GERMANY

Received: March 1, 2018

Accepted: October 15, 2018

Published: November 5, 2018

Copyright: © 2018 García-López et al. This is an open access article distributed under the terms of the [Creative Commons Attribution License](https://creativecommons.org/licenses/by/4.0/), which permits unrestricted use, distribution, and reproduction in any medium, provided the original author and source are credited.

Data Availability Statement: All relevant data are within the paper and its Supporting Information files.

Funding: This work was supported by grants to AB from the Spanish Ministry of Economy, Industry (SAF2015-70882-R; AEI/FEDER, UE), Comunidad Autónoma de Madrid (S2010/BMD-2420), Instituto Salud Carlos III (RETICS TerCel, RD12/0019/0018) and the European Commission (FP7-HEALTH-2009/CARE-MI). AMS was supported by grants

Abstract

Background

Human adult adipose-derived stem cells (hADSCs) have become the most promising cell source for regenerative medicine. However the prolonged *ex vivo* expansion periods required to obtain the necessary therapeutic dose promotes progressive senescence, with the concomitant reduction of their therapeutic potential.

Aim and scope

A better understanding of the determinants of hADSC senescence is needed to improve biosafety while preserving therapeutic efficiency. Here, we investigated the association between deregulation of the imprinted *DLK1-DIO3* region and replicative senescence in hADSC cultures.

Methods

We compared hADSC cultures at short (P_S) and prolonged (P_L) passages, both in standard and low $[O_2]$ (21 and 3%, respectively), in relation to replicative senescence. hADSCs were evaluated for expression alterations in the *DLK1-DIO3* region on chromosome 14q32, and particularly in its main miRNA cluster.

from the MINECO (SAF2010–17167) and Instituto Salud Carlos III (RETICS TerCel, RD12/0019/0013), and MFF and RGU by grants from the Plan Nacional de I+D+I 2013–2016/FEDER (PI15/00892), the Asturias Regional Government (GRUPIN14-052), the IUOPA (Obra Social Cajastur) and the Fundación Científica de la AECC. SGL held a predoctoral fellowship from the Spanish Programa de Formación del Profesorado Universitario.

Competing interests: The authors have declared that no competing interests exist.

Results

Comparison of hADSCs cultured at P_L or P_S surprisingly showed a quite significant fraction (69%) of upregulated miRNAs in P_L cultures mapping to the imprinted 14q32 locus, the largest miRNA cluster described in the genome. In agreement, expression of the lncRNA *MEG3* (Maternally Expressed 3; *Meg3/Gtl2*), cultured at 21 and 3% $[O_2]$, was also significantly higher in P_L than in P_S passages. During hADSC replicative senescence the AcK16H4 activating mark was found to be significantly associated with the deregulation of the entire *DLK1-DIO3* locus, with a secondary regulatory role for the methylation of DMR regions.

Conclusion

A direct relationship between *DLK1-DIO3* deregulation and replicative senescence of hADSCs is reported, involving upregulation of a very significant fraction of its largest miRNA cluster (14q32.31), paralleled by the progressive overexpression of the lncRNA *MEG3*, which plays a central role in the regulation of *Dlk1/Dio3* activation status in mice.

Introduction

Human adipose-derived stem cells (hADSCs) have become an increasingly important cell source in regenerative medicine, as moderate yields can be obtained by minimally invasive techniques from different adipose depots. As the amount of cells obtained by this technique is, nevertheless, limited, *ex vivo* expansion is necessary for downstream clinical use. There is increasing evidence that standard cell culture methods at high $[O_2]$ (atmospheric; 21%) are stressful for several cell lineages, including hADSCs [1–4]. Indeed, in standard conditions, human mesenchymal stem cell (hMSC) cultures progressively evolve towards replicative senescence, with an accelerated rate of telomere erosion and an accumulation of genomic alterations [3–5]. Moreover, hADSC senescence correlates with the progressive loss of stem cell properties that could curtail their therapeutic potential [6–8]. Culture of hMSCs at lower concentrations (3–5%) of $[O_2]$ revealed a significant increase in culture lifespan and better cellular quality, which was associated with a favorable metabolic state of increased glycolysis and decreased oxidative phosphorylation, resulting in reduced levels of oxidative stress [3–8]. In agreement with these observations are the results of several studies using *ex vivo* treatments with antioxidants (reviewed in [9]); for example, short-term treatment of hADSCs with physiological concentrations of zinc sulphate promotes telomere length extension. It is important to note while low $[O_2]$ is usually referred to as hypoxia, low O_2 tensions are considered normoxic in several organs [10,11].

Replicative senescence and aging involves a series of epigenetic alterations such as hypermethylation of specific genomic regions, but against a background of general DNA hypomethylation [12]. This scenario promotes silencing of proliferation-associated genes, whereas tumor suppressor genes are derepressed [13,14]. The main pathways activated in senescent cells are Rb/p16 and p53/21, leading to progressive cell cycle blockade and cell growth arrest. In line with this, the positive effects on hADSCs by short-term treatment with zinc sulphate are mediated by modulation of the methylation status of the promoter of TERT, the telomerase catalytic subunit [9]. Many studies consider senescence as a tumor suppressor network mechanism (reviewed in [15]).

The imprinted *DLK1-DIO3* domain at 14q32.2–32.31 has been associated with regulation of senescence and stem cell function, and is also involved in human cancer [16]. The *DLK1-DIO3* locus is conserved in placental mammals (*Dlk1/Dio3* in mice; located on 12qF1) and is one of the three imprinted loci (with IGF2/H19 and the 15q25.1 locus) that acquire their imprinting through the paternal allele [17,18]. In addition, *DLK1-DIO3* includes the largest cluster of miRNAs described thus far ([19]; see S1 Fig). Concerning senescence, several *DLK1-DIO3* mapping genes, both coding and non-coding, have been previously described to be able to regulate senescence in several cell types; for example, miR-369-5p and miR-485-5p have been shown to be involved in hADSC senescence [13,20,21]. Upregulation of *Dlk1/Dio3* miRNAs has also been implicated in murine lupus, being associated with global DNA hypomethylation, but with differential alterations in several splenic subsets [22]. Also, miR-679 and miR-300 are affected by long-lasting alterations in DNA methylation, as a result of fetal alcohol exposure [23]. In mouse cardiac progenitor cells, however, this correlation was the opposite: miR-300 is positively regulated by *Bmi1*, preventing senescence progression. Furthermore, miR-300 downregulation is required for endothelial and cardiogenic differentiation [24].

MEG3 (maternally expressed 3) is a maternally-expressed, [imprinted long non-coding RNA](#) (lncRNA) gene that maps to the *DLK1-DIO3* locus in humans, whereas the murine homologue (*Meg3/Gtl2*) maps to chromosome 12 [25]. *MEG3* has been extensively associated with multiple human cancer types and is proposed as a tumor suppressor and a negative regulator of angiogenesis [26,27]. Aberrant hypermethylation of the *MEG3* promoter is believed to be the main mechanism involved and its down-regulation is an unfavorable survival factor in bladder cancer [28,29]. *MEG3* has been also found in exosomes from cervicovaginal lavage of cancer patients [30]. Finally, It has been reported that *MEG3* is regulated by the retinoblastoma protein [31] and its forced expression usually suppresses proliferation and promotes apoptosis [32–34]. However, there is scant information on the role of ncRNAs mapping in the *DLK1-DIO3* locus in hADSC biology. In certain pathological conditions, such as the myelodysplastic syndromes, bone marrow hADSCs show an overactivation of the *DLK1-DIO3* locus and have prominent features of senescence, including a highly reduced osteogenic capacity [35]. In multiple myeloma, bone marrow hADSCs also exhibit increased senescence with participation of the overexpressed miR-485-5p, located in the *DLK1-DIO3* region [20].

Here, we have explored the possible association between adult hADSC replicative senescence and alterations in the regulation of the *DLK1-DIO3* locus.

Materials and methods

Human mesenchymal stem cell culture

hADSCs were cultured as described [3]; see Supporting Information.

RT-qPCR analysis

Total RNA was isolated using TriReagent solution (Sigma). Complementary DNA (cDNA) was generated from 1 µg of total RNA using the SuperScript III First-Strand Synthesis System for RT-PCR kit (Invitrogen) in a 20-µl final reaction volume. Real-time PCR reactions were performed using 2 µl/well of a 1/5 dilution of each cDNA and 5 µl of Power SYBR Green PCR Master Mix (Applied Biosystems) in a 10 µl final volume. Results were analyzed using the comparative method ($2^{-\text{ddCt}}$) and normalized to endogenous expression of β -glucuronidase (GUSB).

Microarray hybridization and data analysis

Total RNA extraction from eight biological samples (adult adipose tissue derived: short-term culture ahADSCs, $n = 2$ biological replicates; long-term culture ahADSCs, $n = 2$; pediatric adipose tissue-derived phADSCs, $n = 3$; long-term culture phADSCs, $n = 1$) was performed with the mirVana miRNA Isolation Kit (Applied Biosystems). Samples were hybridized to the human miRNA Microarray v1.0 (Agilent Technologies) and processed as indicated. miRNA data was normalized based on the VSN-invariant method. From a total of 721 human sequences, after normalization, only those probes with an average expression above the 20th percentile of all average expressions (393 miRNAs) were considered for analysis. The *Limma* package was used to determine differentially expressed miRNAs, and we focused on those miRNAs with an adjusted p -value < 0.2 . miRNA data are accessible in the Gene Expression Omnibus (GEO) database repository (GSE121481).

DNA methylation analysis

Genomic DNA was isolated using TriReagent solution and modified by sodium bisulfite conversion as described [36]. Briefly, 1 μ g of genomic DNA was denatured with a final concentration 0.3 M NaOH at 37°C for 10 minutes. Denatured DNA was then treated with a final concentration of 2.6 M bisulphite/0.5 mM hydroquinone mixture, at 50°C for 16–18 hours, protected from light. Treated DNA was cleaned with the Wizard DNA clean-up system (Promega). Eluted samples were then treated with NaOH as above, and then ethanol-precipitated. PCR was performed on bisulfite-treated DNA, and PCR products were cloned into the pGEM-T-Easy vector (Promega) and sequenced. To examine the methylation status of the IG-DMR and MEG-DMR, three and five clones, respectively, were analyzed for each condition. PCR primers are listed in Supplementary S4 Table and were previously reported [37]. Sequencing results were analyzed using CpGViewer software.

Chromatin immunoprecipitation

Chromatin immunoprecipitation (ChIP) was performed as described [10]. Briefly, cultured cells were fixed with 1% formaldehyde and crosslinking was terminated by the addition of glycine to a final concentration of 125 mM. Cells were washed twice in cold PBS with protease inhibitors, scraped, collected, pelleted and resuspended in SDS lysis buffer (1% SDS, 10 mM EDTA, 50 mM Tris pH 8). Chromatin was fragmented using the Bioruptor Sonication System (Diagenode). Samples were immunoprecipitated using anti-IgG (ab46540, Abcam), -AcK16H4 (07–329, Millipore) or -total H3 antibodies (ab1791, Abcam). Samples were analyzed by quantitative PCR. Nonspecific adjustment (dCq) was calculated by ($dCq = Cq_{[IP]} - Cq_{[IgG]}$). Fold enrichment was calculated as $2^{-(ddCq)}$, where $ddCq$ is calculated by ($ddCq = Cq_{[PL]} - Cq_{[PS]}$).

Results

MEG3 expression is deregulated by replicative senescence in human ADSCs

We sought to compare the effects of standard (21% [O₂]) versus normoxic (3% [O₂]) conditions in prolonged (≥ 20 passages; but variable with the individual isolates) cultures of adult hADSCs (P_L) and short (≤ 12 passages; P_S) passages, in relation to the concurrent replicative senescence previously described [3–6]. We first confirmed that cell culture growth rate was higher at 3% [O₂] than at 21% [O₂] (Fig 1A, S1A and S1B Fig). Analysis of hADSCs grown at 21% [O₂] or 3% [O₂] showed that long passages led to a decreased capacity for differentiation

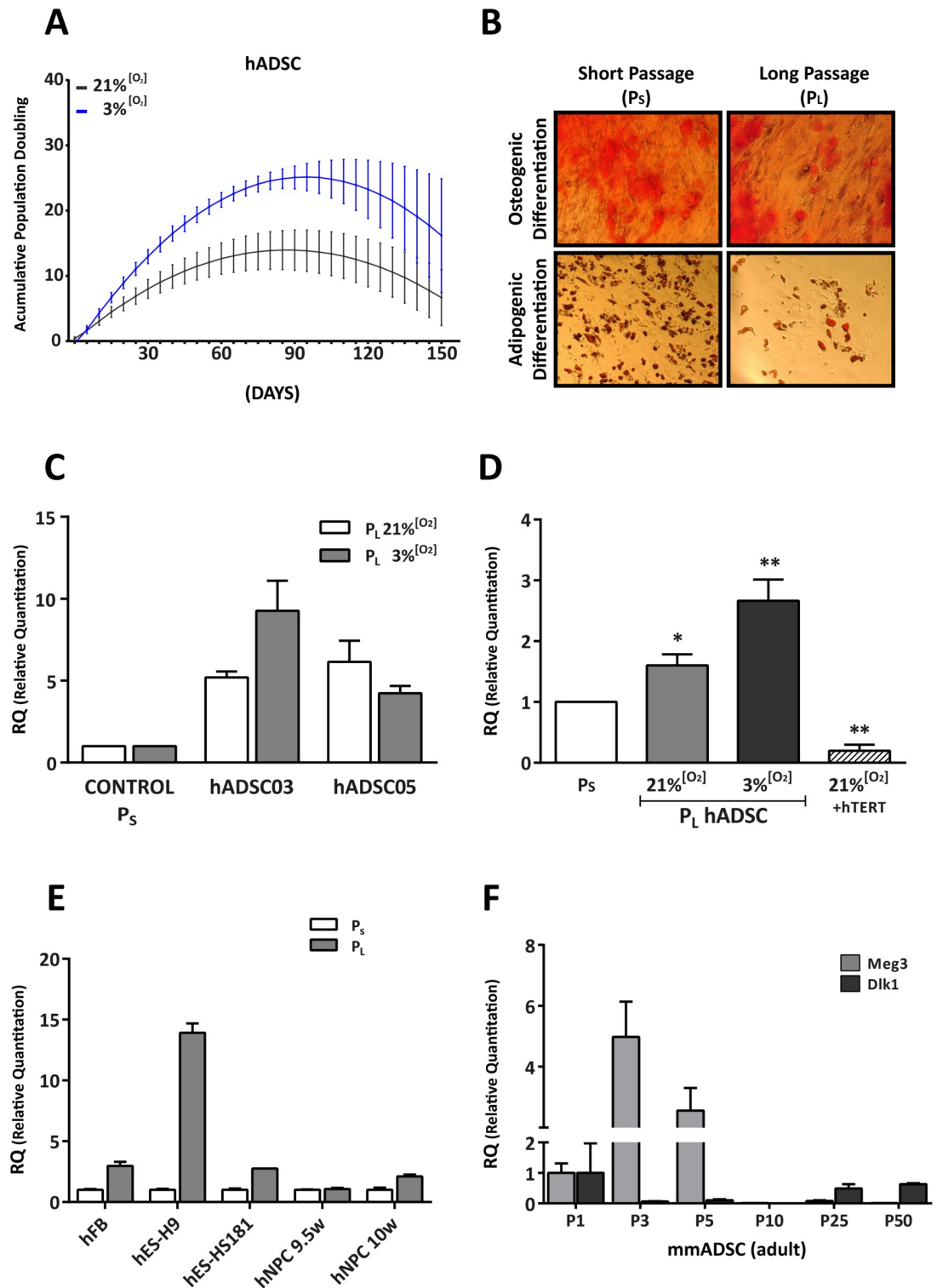


Fig 1. Replicative senescence is associated with upregulated lncRNA *MEG3* expression. (A) Model of hADSC proliferation kinetics. From the cumulative population doubling data for different hADSC cultures, we obtained a curve fitted to a polynomial function that modeled hADSC proliferation kinetics. The various hADSC cultures were used to establish a mean proliferation curve for 150 days. Each dot represents the mean \pm SEM of data obtained by modeling the different hADSC cultures. (B) Representative images indicating loss of differentiation potential (adipogenic and osteogenic) in P_l cultures as compared with P_s cultures of hADSCs. (C) Relative quantitation of *MEG3* lncRNA in two different hADSC samples ($n = 3$ technical replicates)

cultured for short (P_S) and long (P_L) periods. Data shown represent mean \pm SEM. (D) Relative quantitation of *MEG3* expression in P_S and P_L hADSC cultures from a different source, Inbiobank (aADSC, $n = 4$ biological replicates; with overexpressed hTERT; +hTERT, $n = 2$ biological replicates); data represent mean \pm SEM (* $p < 0.05$, ** $p < 0.01$, *** $p < 0.001$; two-tailed paired t-test). (E) Relative quantitation of *MEG3* expression in different cell models (hFB, human fibroblasts; hES-H9, human embryonic stem cell H9; hES-HS181, human embryonic stem cell HS181; hNPC 9.5w, human neural precursor cells from a 9.5-week fetus; hNPC 10w, human neural precursor cells from a 10-week fetus); shown is a representative experiment with 3 technical replicates. (F) Relative quantitation of *Meg3* and *Dlk1* expression in mouse ADSCs (mADSCs) at various passages; shown is a representative experiment with 3 technical replicates. Data represent mean \pm SEM.

<https://doi.org/10.1371/journal.pone.0206534.g001>

(Fig 1B), to an increase in cell size and complexity (S1C Fig) and cellular morphology changes as well as SA- β -gal positive staining (S1D Fig), as previously reported [3,4].

Because of the central role proposed for lncRNA *MEG3* in the regulation of the *Dlk1/Dio3* (S1E Fig) locus activation status in mouse [38], we investigated its potential deregulation with regards to replicative senescence in hADSCs. RT-qPCR analysis of *MEG3* expression in hADSCs cultured at 21 and 3% $[O_2]$ showed that *MEG3* expression was significantly higher in P_L than in P_S cultures (Fig 1C and 1D). To confirm the possible association of *MEG3* upregulation with replicative senescence, we analyzed the effect of constitutive expression (lentiviral transduction) of the telomerase catalytic subunit TERT, which hinders or prevents cell senescence in hADSCs [3,4]. The *MEG3* overexpression observed in P_L samples was significantly diminished in hADSCs expressing TERT, with levels below those found in P_S cultured hADSCs (Fig 1D). These data suggest that mechanisms involved in regulation of *MEG3* expression at the *DLK1-DIO3* locus are associated with replicative senescence. We also evaluated the behavior of another imprinted locus, *IGF2*, finding that its expression was also upregulated in P_L samples, and constitutive TERT expression prevented or counteracted this upregulation (S2A Fig). Overall, these findings suggest that multiple imprinted loci can be similarly affected during hADSC proliferative senescence.

To determine whether deregulation of the *DLK1-DIO3* locus could be a general feature of cell senescence, we analyzed *MEG3* expression in P_L and P_S cultures of several human cell lineages (Fig 1E). Similar to that found for hADSCs, *MEG3* was upregulated in human fibroblasts (hFBs) with cell passage. The human ES cell lines tested (H9, H181) showed large differences in *MEG3* expression after several passages, likely reflecting their heterogeneity, but both increased their levels of *MEG3* with progressive passaging. By contrast, neural progenitor cells (hNPCs) [39,40] showed discrete *MEG3* overexpression. Also, some v-myc-immortalized derivatives showed strong *MEG3* downregulation as compared with non-immortalized samples (S2B Fig). Because v-myc induces telomerase activity in hNPC lines [39,40] these results are compatible with our findings in hADSCs after hTERT overexpression (Fig 1D). In murine ADSCs, *Meg3* was upregulated in early passages (P_2 – P_5) and then decreased significantly (Fig 1F), doubtless coupled to the culture growth crisis before immortalization. At later stages (P_{25} –50), *Meg3* was re-expressed at a lower level relative to initial levels. Finally, expression of murine *Dlk1* (delta like non-canonical Notch ligand 1), also mapping in locus *Dlk1/Dio3*, did not parallel this profile (Fig 1F). In conclusion, our results suggest that upregulation of *MEG3* in association with replicative senescence seems to be a phenomenon mostly restricted to human primary adult cells, both hADSCs and hFBs.

14q32.31 miRNA cluster expression is globally altered by replicative senescence in human ADSCs

The significant alteration in *MEG3* expression prompted us to characterize the miRNA repertoire associated with replicative senescence in hADSCs. We focused mainly on the 14q32.31 miRNA cluster, the largest described in the genome (reviewed in [19]). hADSCs were cultured

at 3% [O₂], with the aim to reduce the artificial oxidative stress background generated by higher [O₂]. The distribution of the normalized intensity of miRNA array data of hADSCs in P_L versus P_S cultures is depicted in [S3A Fig](#). Statistical analysis identified 84 miRNAs (21.3%) differentially expressed in P_L versus P_S ([S1 Table](#)). Among the downregulated miRNAs [[41](#)], at least four members of the miR-17-92a cluster were identified ([S1 Table](#)). Interestingly, members of this cluster are oncomiRs, and their downregulation is associated with cell senescence and aging [[14,41](#)].

One significantly upregulated miRNA was miR-34a, which is considered a tumor suppressor and is reported to repress targets involved in cell cycle, apoptosis and senescence, following p53-induced transactivation [[42,43](#)]. Several other upregulated miRNAs found in our analysis have also been associated with cell senescence and aging [[13,41](#)]. Surprisingly, a quite significant fraction (69%) of upregulated miRNAs in hADSC P_L cultures ([Fig 2A](#) and [S1 Table](#)) mapped to the imprinted 14q32 locus ([S1D Fig](#)). Proportion statistical test analysis confirmed that the upregulated miRNA fraction in this region was significantly greater than that expected by chance ($p < 0.0001$), therefore strongly suggesting a marked upregulation of the locus associated with replicative senescence. To clarify whether these changes could be associated with chronological aging, we performed a similar analysis in hADSCs obtained from pediatric (<15-year-old donors; phADSCs) that demonstrated a comparable *in vitro* behavior. After data normalization, all miRNAs of the 14q32 locus included in the miRNA array were found to be deregulated, with a predominant tendency to upregulation ([S4A Fig](#)).

We selected miR-369-5p, miR-136 (which maps to 14q32; [S1 Table](#)) and miR-34a (mapping in 1p36.22), involved in senescence and tumor suppression [[44,45](#)] for quantitative RT-qPCR validation analysis. In independent batches of P_L cultured hADSCs, we confirmed that all three miRNAs were upregulated in 3% [O₂], both in adult and pediatric ADSCs, as compared with P_S cultures ([Fig 2B](#), [S3](#) and [S4 Figs](#)). To exclude major alterations in the miRNA biogenesis machinery as a secondary cause of general miRNA upregulation in the 14q32 region during replicative senescence, we evaluated the expression of *DICER* after long-term cell culture periods at 21% or 3% [O₂], and with both hADSCs populations, finding no significant reduction in its expression ([S4C Fig](#)). These findings strongly suggest a deregulated 14q32 miRNA expression pattern is associated with replicative senescence in P_L hADSC cultures.

Deregulation of the 14q32 locus in long-term-cultured hADSCs is partially mediated by epigenetic modifications

Two main differentially methylated regions (DMRs) have been reported in the 14q32 locus: both intergenic (IG)-DMR and *MEG*-DMR ([S1E Fig](#)) can behave as imprinting control regions to regulate monoallelic expression of 14q32 locus clustered genes [[46, 47](#)]. To determine whether *MEG3* and miRNA upregulation are mediated by epigenetic modification *via* DNA methylation, we performed bisulfite-sequencing analysis on hADSCs grown at 3% [O₂].

Surprisingly, the CpG methylation pattern of the individual clones analyzed to study IG-DMR showed considerable methylation heterogeneity (data not shown), which was unexpected for a DMR region. Moreover, the IG-DMR region showed no consistent differences in the hADSC samples under any experimental condition (P_L/P_S), even though there was a tendency for increased methylation with passages when the CpGs of the region were analyzed individually ([Fig 3A](#)).

In the *MEG*-DRM DNA methylation analysis, we observed a methylation pattern of the different analyzed clones consistent with those expected from a DMR region ([Fig 3B](#)). As was the case for IG-DMR, the analysis of the *MEG*-DMR region showed no significant P_L/P_S differences in CpG methylation status in samples cultured to senescence ([Fig 3A](#)), even though

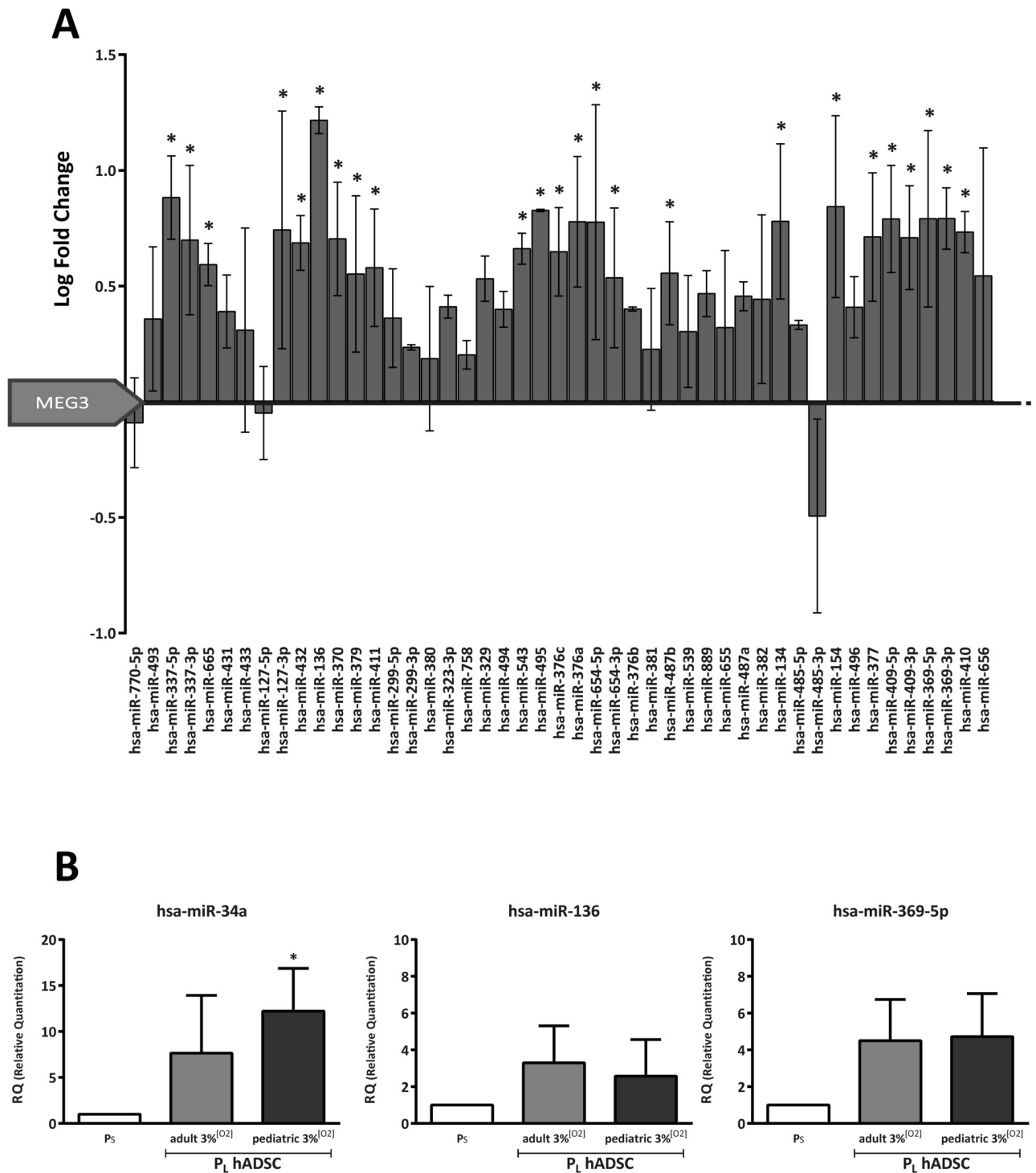


Fig 2. miRNA 14q32.31 cluster is deregulated in association with replicative senescence. (A) Bar graph shows log fold-change expression for the miRNAs in the 14q32 chromosome region that were deregulated in short-term (P_S) versus long-term (P_L) cultured adult ADSC samples ($n = 2$ biological replicates in both cases; mean \pm SEM). (B) Relative quantitation (see extended methods in Supporting information for details) of selected miRNAs for array validation in adult ($n = 3$ biological replicates) and pediatric ($n = 2$ biological replicates) hADSCs; data represent mean \pm SEM (* $p < 0.05$; one-tailed paired t-test).

<https://doi.org/10.1371/journal.pone.0206534.g002>

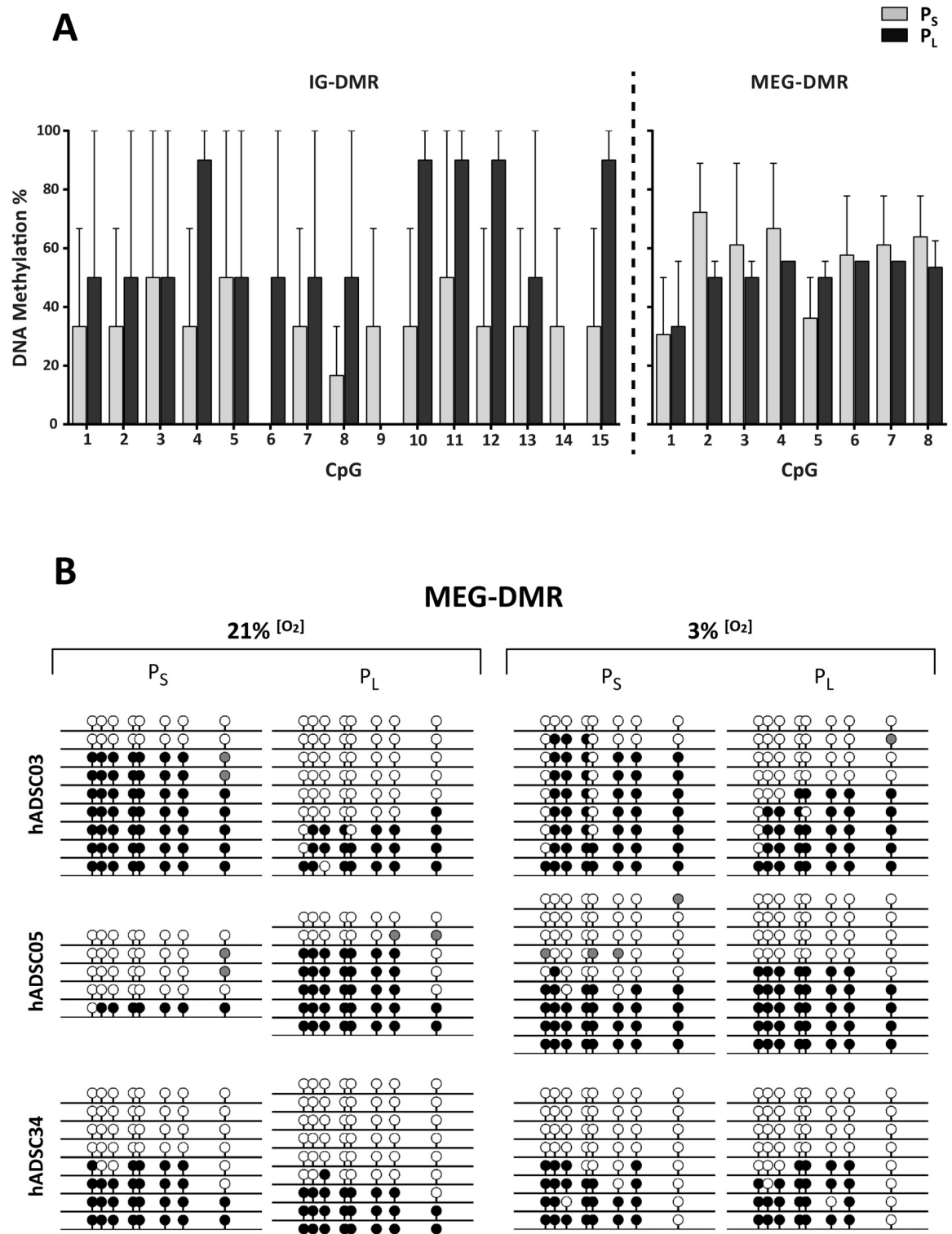


Fig 3. DNA methylation analysis of *DLK1-DIO3* IG- and *MEG*-DMR regions. (A) Percentage of DNA methylation in hADSC samples; x-axes indicate the CpG analyzed in the IG-DMR (1–15) and in the *MEG*-DMR region (1–8). Data represent mean \pm SEM for P_S and P_L cultures. (B) Bisulfite genomic sequencing of the *MEG*-DMR regions. CpG dinucleotides are represented as lollipops; methylated cytosines, black; unmethylated cytosines, white. Cultures grown at 21% or 3% [O₂] (P_S vs. P_L) were compared for the indicated hADSC samples.

<https://doi.org/10.1371/journal.pone.0206534.g003>

individual CpG analysis showed a moderate tendency of decreased methylation with passages. Indeed, only the hADSC03 cell isolate cultured to senescence showed a clear DNA demethylation of the *MEG3*-DMR region. To establish whether the effect observed in the *MEG3*-DMR was due to the oxygen tension, we repeated the DNA methylation analysis on hADSC samples cultured to senescence under 21% [O₂]. In this case we observed similar results for *MEG3*-DMR to those observed in 3% [O₂] cultures (Fig 3B).

Analysis of the main enzymes of the methylation machinery (DNMT1, DNMT3a and DNMT3b) showed no significant modification in their gene expression, with the exception of *DNMT3a* whose expression was significantly decreased in P_L ADSC cultures (Fig 4A). Globally, although hADSCs treated with the DNMT inhibitor 5-aza-2'-deoxycytidine (AZA) demonstrated increased *MEG3* expression (S4 Fig), the results suggested no direct correlation between hADSC replicative senescence and DNA methylation in the analyzed regions for IG- and *MEG3*-DMR.

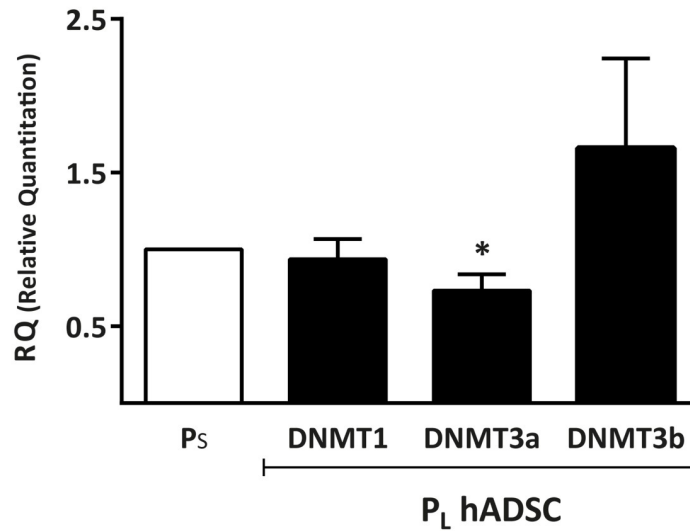
We then explored other epigenetic modifications potentially involved in the upregulation of the 14q32 locus non-coding genes. Treatment of hADSCs with trichostatin A (TSA), a histone deacetylase inhibitor, significantly increased *MEG3* expression both at P_L and P_S (S4D Fig), suggesting the involvement of histone deacetylation in regulating *MEG3* expression during senescence. We therefore carried out ChIP to study distribution of an activating acetylation mark (AcK16H4) in different regulatory sequences of the *DLK1-DIO3* locus, comparing P_L and P_S at 3% [O₂]. The results showed that the acetylated K16H4 mark was enriched (30- to 75-fold) in P_L hADSCs, relative to P_S hADSCs, in most segments tested (D1, M1, M3); the M2 segment was also enriched, but at a lower level (Fig 4B). Segment D1 is upstream of *DLK1*-DMR, and segments M1–M3 are found in *MEG3* and upstream of the miRNA cluster (see S1 Fig). Overall, these findings suggest that the AcK16H4 activating mark is significantly associated with the upregulation of the entire *DLK1-DIO3* locus during hADSC replicative senescence.

Discussion

The *DLK1-DIO3* imprinted locus has attracted much attention because it is one of the few loci critically altered during generation of murine and human induced pluripotent stem cells [48, 49]. Expression of coding and non-coding genes of the *Dlk1-Dio3* imprinted cluster (*Gtl2/Meg3*, miR-127, miR-134 and miR-154) is deregulated due to aberrant DNA methylation of the maternal allele, whereas the paternal allele preserves a normal methylation status [38]. Preservation of *Dlk1-Dio3* imprinting is improved by Dppa3/Pgc7 (developmental pluripotency-associated protein 3) binding to discrete domains of the IG-DMR region, and competing with Dnmt3a to preserve the original imprinting [49]; Polycomb Repressive Complex 2 (PRC2) is also a key element in maintaining expression of maternal miRNA and lncRNA from the *Dlk1-Dio3* locus [38]. More recently, it has been demonstrated that IG-DMR acts as an enhancer for the entire locus and that PRC2 interacts physically with *Gtl2/Meg3* and Dnmt3 methyltransferase, reducing methylation at the IG-DMR [50]. Interestingly, it has also been recently reported that several ncRNAs corresponding to the *Gtl2/Meg3* domain, including *Gtl2*, are enriched in the murine hematopoietic stem cell pool (HSC; CD49b^{lo}). These ncRNAs regulate activation of the PI3K-mTOR pathway and mutant HSCs (IG-DMR deletion) presented increased mitochondrial biogenesis, metabolic activity and ROS levels [51]. Therefore, it can be tentatively concluded that a balanced cell-specific expression of the *Dlk1-Dio3* locus is essential for optimal functional maintenance of pluripotent, fetal and adult stem cells.

Our work on replicative senescence in hADSCs revealed also an important role for the imprinted *DLK1-DIO3* locus. Several studies show that low oxygen concentrations (3% [O₂]),

A



B

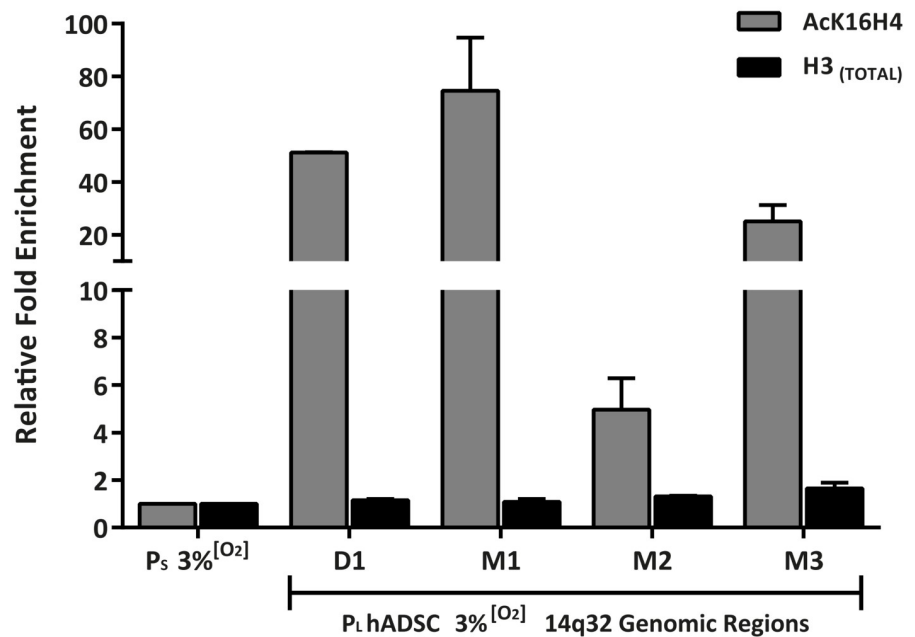


Fig 4. Epigenetic analysis of DLK1-DIO3 DMR regions. (A) Relative quantitation of *DNMT1*, *DNMT3a* and *DNMT3b* (hADSCs; $n = 5$ biological replicates). Data represent mean \pm SEM (* $p < 0.05$; two-tailed paired t-test). (B) Fold enrichment of AcK16H4 relative to total H3 in hADSC05 cultured at 3% [O₂], comparing P_S and P_L samples. Enriched DNA was analyzed by qPCR using primers specific for the different regions (D1, M1–M3; see S1 Fig and S4 Table). Nonspecific adjustment (dCq) was calculated by (dCq = Cq_[IP] – Cq_[IGC]). Fold enrichment was calculated as $2^{-(ddCq)}$ where ddCq is (ddCq = Cq_[PL] – Cq_[PS]).

<https://doi.org/10.1371/journal.pone.0206534.g004>

significantly lower than atmospheric (21% [O₂] pressure) improve the proliferation rate and quality of myriad tissue-derived cell cultures. In hADSCs, it was demonstrated that low oxygen concentrations reduce the senescence ratio during expansion [2–5]. Our results indicate that expanded hADSCs (both at 21 or 3% [O₂], and using adult or pediatric isolates) present a progressive increase in *MEG3* expression, and this effect could be reverted by constitutive expression of the TERT catalytic subunit. *MEG3* has been proposed as a tumor suppressor and a negative regulator of angiogenesis [30,31], and its down-regulation serves as an unfavorable risk factor for survival in multiple human cancer types [32–34], mainly by promoter and IG-DMR region hypermethylation [52]. Interestingly, it has been proposed to also act as a competing endogenous RNA for several miRNAs (sponging), including miR-15a-5p, miR-19a, miR-664 and miR-214 [53]. In addition, it is interesting to note that trans-associations between the IGF2, *MEG3* and *DLK1* imprinted gene products have been proposed and that their three-dimensional nuclear organization is linked to the transcriptional state of these genes [54]. These findings suggest that during adult ADSC proliferative senescence, multiple imprinted loci could co-operatively be affected.

In addition, our miRNA analysis demonstrated that a quite significant fraction (69%) of senescence-upregulated miRNAs map also in the 14q32.31 cluster, involving miRNAs previously associated with senescence. For example, miR-136 is linked to fibroblast senescence, promoting apoptosis in glioma cells by targeting several anti-apoptotic genes [55], and miR-369-5p has previously been associated with hADSC senescence [13,21]. This means that the 14q32.31 miRNA cluster response is the major miRNA cellular response associated with replicative senescence. Comparison of our results with those of a previous study of radiation-induced senescence in hADSC [6] confirmed upregulation of some of the miRNAs identified here (e.g., miR-629-3p and miR-34a-5p). In agreement, *in silico* analysis of the putative target genes for senescence-deregulated miRNAs of the 14q32.31 locus (S2 Table; >1400 genes) highlighted biological functions involved in cell aging, gene expression, cell cycle and apoptosis (S3 Table). Several of these genes have been also identified as age-associated [56]. One of the clearest hallmarks of senescent hADSCs is a marked decrease in expression of AP-1 components (FOS and JUN, and their phosphorylated forms), which are critically associated with mobility and responsiveness limitation [6]. In the context discussed here, FOS is a significant target of miR-543 and miR-221, both up-regulated by senescence, and mapping in the 14q32.31 miRNA cluster. Finally, and in close agreement with the interpretation of our data, a recent study identified as tumor suppressors 26 targets for the entire 14q32.31 miRNA cluster [57].

The progressive and significant up-regulation of *MEG3* and 14q32.31 miRNA cluster (the largest described so far, with up to 54 described miRNAs) expression could have a significant pleiotropic effect, suppressing proliferation and promoting apoptosis/senescence of hADSCs. Comparing the evidence obtained in senescent hADSCs with that in reprogramming schemes in adult cells [43–45] or in murine hematopoietic stem cells [46], it is clear that during replicative senescence of hADSCs, alterations in expression regulation are not dominated by a strong differential methylation of the main DMRs regulatory regions, although a compatible down-regulation of *DMT3A* was found (Fig 4A). On the contrary, histone acetylation on specific domains seems to play a more decisive role. That said, a significant proportion of the miRNAs affected by IG-DMR deletion [51] are also found upregulated in senescent hADSCs (S1 Table), showing differences and similarities in those processes, all connected by the complex regulation of the imprinted *DLK1-DIO3* locus. During hADSC replicative senescence, there is progressive accumulation of *MEG3* expression that, based on the known regulatory features of the *Dlk1-Dio3* locus [44,49], could generate a feedback activation loop to promote and/or maintain IG-DMR overactivation. Given the central role proposed for *Gtl2/Meg3* as an enhancer of

the *Dlk1-Dio3* locus, we speculate that these regulatory mechanisms could be altered during hADSC senescence, but not critically related to methylation.

Conclusions

Our data strongly support a direct relationship between *DLK1-DIO3* (14q32) deregulation and replicative senescence of hADSCs. We found a specific profile that includes progressive upregulation of *DLK1-DIO3*-encoded lncRNA *MEG3* expression and upregulation of a very significant fraction of its largest miRNA cluster (14q32.31). Both of these main features are associated with tumor suppression and a putative correlation has been also proposed between *MEG3* upregulation and physiological aging and replicative senescence of stem and progenitor cells [58–60]. This is consistent with the idea that senescence is primarily a tumor suppressor mechanism and that progressive hyperactivation of the *DLK1-DIO3* cluster is thus likely a potent concerted tumor suppressor network. Altered expression of *MEG3* is not mainly associated with methylation levels in DMR domains, but to an increase in histone activation marks in discrete domains.

Supporting information

S1 Fig. Loss of hADSC biological properties in long-term culture. (A) Model of hADSC proliferation kinetics. From the cumulative population doubling data for different hADSC cultures, we obtained a curve fitted to a polynomial function. The various hADSC cultures were used to establish a mean proliferation curve for 150 days. Each dot represents the mean \pm SEM of data obtained by modeling the different hADSC cultures. (B) Percentage of cells in cell cycle phase G_0/G_1 at different cell culture stages (hADSCs, $n = 4$ biological replicates); the graph shows the mean \pm SEM of different cell cultures (* $p < 0.05$; two-tailed paired t-test). (C) Representative FSC-A/SSC-A plot diagrams, representing cell size and complexity in P_S and P_L hADSC cultures. (D) Light microscopy image exemplifying senescent morphology changes and SA- β -gal staining of senescent (P_S) cell cultures. (E) Scheme of the imprinted 14q32.2-14q32.31 locus, including the regions analyzed by bisulfite genomic sequencing (BS), and by ChIP of AcK16H4; coding genes are shown as black boxes, non-coding genes as gray boxes and miRNAs as triangles.
(TIF)

S2 Fig. Analysis of replicative senescence on *IGF2* expression in hADSCs and v-myc immortalized NSCs. (A) Relative quantitation of *IGF2* in hADSCs ($n = 4$ biological replicates; obtained from Inbiobank) and in hADSCs overexpressing hTERT (+hTERT; $n = 2$ biological replicates). (B) Relative quantitation of *MEG3* in v-myc-immortalized human NPCs ($n = 3$ technical replicates); data represent mean \pm SEM (* $p < 0.05$, ** $p < 0.01$, *** $p < 0.001$; two-tailed paired t-test).
(TIF)

S3 Fig. Analysis of adult hADSCs. (A) Scatter plot showing distribution of the VSN-invariant normalized intensity data for short-term (P_S) and long-term cultured (P_L) hADSC samples ($n = 3$ biological replicates). (B) Relative quantitation of selected miRNAs for array validation in the samples used for the array expression assay; hADSC P_S and P_L samples ($n = 3$ biological replicates). Cultures were grown at 3% $[O_2]$.
(TIF)

S4 Fig. Analysis of pediatric hADSCs. (A) Bar graph showing array data analysis as log fold-change expression in pediatric hADSCs (mean \pm SEM) of all miRNAs in the 14q32 chromosome region analyzed. (B) Relative quantitation of *DICER* in hADSCs ($n = 5$ biological

replicates) and pediatric hADSCs ($n = 9$ biological replicates) expanded both at 3% and 21% [O₂]. (C) Relative quantitation of lncRNA *MEG3* in pediatric hADSC samples (P_S and P_L), cultured at 21% [O₂], treated or not (control) with epigenetic drugs; gray bars indicate samples analyzed at 72 h after TSA or 5-AZA treatments and gray stippled bars correspond to samples treated with drugs for 72 h, washed, recultured and analyzed after an additional 96 h. Bars represent mean \pm SEM ($n = 2$ technical replicates) * $p < 0.05$; two-tailed ratio paired t-test. (TIF)

S1 Table. miRNAs differentially expressed in short-term versus long-term hADSC cultures. Upregulated miRNAs shadowed in pale green correspond to those described as upregulated in HSC (CD49b^{lo}) [56], controlling PI3K-mTOR pathway. (PDF)

S2 Table. miRNA predicted targets. Table compiles 1,478 predicted targets (see [Materials and methods](#)) of the deregulated miRNAs identified in array experiments, indicating those mRNAs that are predicted as targets for multiple miRNAs. (PDF)

S3 Table. GO analysis of validated targets of *DLK1-DIO3*-upregulated miRNAs. (DOCX)

S4 Table. List of primers used in the study. (TIF)

S1 File. Garcia-Lopez et al. PlosOne_SUPP. Extended methods. (DOCX)

Acknowledgments

We thank Drs M Ramírez (Hospital Niño Jesús, Madrid), D García-Olmo (Hospital La Paz, Madrid), and M Lamana and R Yáñez (CIEMAT, Madrid) for help in collecting human and murine ADSC samples. We also thank Drs Enrique Samper and Juan C Estrada (CNIC, Madrid) for provision of TerT-hADSC. We acknowledge Drs MP Pereira (CBMSO, Madrid) for helpful comments and suggestions and C Mark and K McCreath for editorial assistance. SGL held a predoctoral fellowship from the Spanish Programa de Formación del Profesorado Universitario.

Author Contributions

Conceptualization: Silvia García-López, Antonio Bernad.

Formal analysis: Silvia García-López, Fátima Sánchez-Cabo.

Funding acquisition: Alberto Martínez-Serrano, Mario F. Fraga, Antonio Bernad.

Investigation: Silvia García-López, Carmen Albo-Castellanos, Rocio G. Urduñigo, Susana Cañón, Alberto Martínez-Serrano, Mario F. Fraga, Antonio Bernad.

Methodology: Silvia García-López, Carmen Albo-Castellanos, Antonio Bernad.

Supervision: Antonio Bernad.

Writing – original draft: Silvia García-López, Antonio Bernad.

Writing – review & editing: Silvia García-López, Susana Cañón, Alberto Martínez-Serrano, Mario F. Fraga, Antonio Bernad.

References

1. Parrinello S, Samper E, Krtolica A, Goldstein J, Melov S, Campisi J. Oxygen sensitivity severely limits the replicative lifespan of murine fibroblasts. *Nat Cell Biol.* 2003; 5:741–7. <https://doi.org/10.1038/ncb1024> PMID: 12855956
2. Busutil RA, Rubio M, Dollé ME, Campisi J, Vijg J. Oxygen accelerates the accumulation of mutations during the senescence and immortalization of murine cells in culture. *Aging Cell* 2003; 2:287–94. <https://doi.org/10.1046/j.1474-9728.2003.00066.x> PMID: 14677631
3. Estrada JC, Albo C, Benguría A, Dopazo A, López-Romero P, Carrera-Quintanar L, et al. Culture of human mesenchymal stem cells at low oxygen tension improves growth and genetic stability by activating glycolysis. *Cell Death Differ.* 2012; 9:743–755.
4. Estrada JC, Torres Y, Benguría A, Dopazo A, Roche E, Carrera-Quintanar L, et al. Human mesenchymal stem cell-replicative senescence and oxidative stress are closely linked to aneuploidy. *Cell Death Dis.* 2013; 4:e691. <https://doi.org/10.1038/cddis.2013.211> PMID: 23807220
5. Gronthos S, Zannettino AC, Hay SJ, Shi S, Graves SE, Kortessidis A, et al. Molecular and cellular characterisation of highly purified stromal stem cells derived from human bone marrow. *J Cell Sci.* 2003; 116:1827–35. PMID: 12665563
6. Sepúlveda JC, Tomé M, Fernández ME, Delgado M, Campisi J, Bernad A, et al. Cell senescence abrogates the therapeutic potential of human mesenchymal stem cells in the lethal endotoxemia model. *Stem Cells* 2014; 32:1865–77. <https://doi.org/10.1002/stem.1654> PMID: 24496748
7. Kim J, Kang JW, Park JH, Choi Y, Choi KS, Park KD, Baek DH, et al. Biological characterization of long-term cultured human mesenchymal stem cells. *Arch Pharm Res.* 2009; 32:117–26. <https://doi.org/10.1007/s12272-009-1125-1> PMID: 19183884
8. Noer A, Lindeman LC, Collas P. Histone H3 modifications associated with differentiation and long-term culture of mesenchymal adipose stem cells. *Stem Cells Dev.* 2009; 18:725–36. <https://doi.org/10.1089/scd.2008.0189> PMID: 18771397
9. Farahzadi R, Fathi E, Mesbah-Namin SA, Zarghami N. Zinc sulfate contributes to promote telomere length extension via increasing telomerase gene expression, telomerase activity and change in the *TERT* gene promoter CpG island methylation status of human adipose-derived mesenchymal stem cells *PLoS One.* 2017; 12(11): e0188052. <https://doi.org/10.1371/journal.pone.0188052> PMID: 29145503
10. Lara E, Mai A, Calvanese V, Altucci L, Lopez-Nieva P, Martinez-Chantar ML, et al. Salermide, a Sirtuin inhibitor with a strong cancer-specific proapoptotic effect. *Oncogene* 2009; 28:781–91. <https://doi.org/10.1038/onc.2008.436> PMID: 19060927
11. Haque N, Rahman MT, Abu Kasim NH, Alabsi AM. Hypoxic culture conditions as a solution for mesenchymal stem cell based regenerative therapy. *Scientific World Journal* 2013;632972. <https://doi.org/10.1155/2013/632972> PMID: 24068884
12. Fernández AF, Bayón GF, Urduñigo RG, Toraño EG, García MG, Carella A, et al. H3K4me1 marks DNA regions hypomethylated during aging in human stem and differentiated cells. *Genome Res.* 2015; 25:27–40. <https://doi.org/10.1101/gr.169011.113> PMID: 25271306
13. Wagner W, Horn P, Castoldi M, Diehlmann A, Bork S, Saffrich R, et al. Replicative senescence of mesenchymal stem cells: a continuous and organized process. *PLoS One* 2008; 3 e2213. <https://doi.org/10.1371/journal.pone.0002213> PMID: 18493317
14. Hong L, Lai M, Chen M, Xie C, Liao R, Kang YJ, et al. The miR-17-92 cluster of microRNAs confers tumorigenicity by inhibiting oncogene-induced senescence. *Cancer Res.* 2010; 70:8547–57. <https://doi.org/10.1158/0008-5472.CAN-10-1938> PMID: 20851997
15. Campisi J, 2005. Suppressing cancer: the importance of being senescent. *Science* 2005; 309:886–7. <https://doi.org/10.1126/science.1116801> PMID: 16081723
16. Benetatos L, Vartholomatos G, Hatzimichael E. DLK1-DIO3 imprinted cluster in induced pluripotency: landscape in the mist. *Cell Mol Life Sci.* 2014; 71:4421–30. <https://doi.org/10.1007/s00018-014-1698-9> PMID: 25098353
17. Wylie AA, Murphy SK, Orton TC, Jirtle RL. Novel imprinted DLK1/GTL2 domain on human chromosome 14 contains motifs that mimic those implicated in IGF2/H19 regulation. *Genome Res.* 2000; 10:1711–8. PMID: 11076856
18. Peters J. The role of genomic imprinting in biology and disease: an expanding view. *Nat Rev Genet.* 2014; 15:517–30. <https://doi.org/10.1038/nrg3766> PMID: 24958438
19. Benetatos L, Voulgaris E, Vartholomatos G. DLK1-MEG3 imprinted domain microRNAs in cancer biology. *Crit Rev Eukaryot Gene Expr.* 2012; 22:1–15. PMID: 22339656
20. Berenstein R, Blau O, Nogai A, Waechter M, Slonova E, Schmidt-Hieber M et al. Multiple myeloma cells alter the senescence phenotype of bone marrow mesenchymal stromal cells under participation of the

- DLK1-DIO3 genomic region. *BMC Cancer* 2015; 15:68. <https://doi.org/10.1186/s12885-015-1078-3> PMID: 25886144
21. Maes OC, Sarojini H, Wang E. Stepwise up-regulation of microRNA expression levels from replicating to reversible and irreversible growth arrest states in WI-38 human fibroblasts. *J Cell Physiol.* 2009; 221:109–19. <https://doi.org/10.1002/jcp.21834> PMID: 19475566
 22. Dai R, Lu R, Ahmed SA. The Upregulation of Genomic Imprinted DLK1-Dio3 miRNAs in Murine Lupus Is Associated with Global DNA Hypomethylation. *PLoS One* 2016; 11(4):e0153509. <https://doi.org/10.1371/journal.pone.0153509> PMID: 27070142
 23. Laufer BI, Mantha K, Kleiber ML, Diehl EJ, Addison S, Shiva M, et al. Long-lasting alterations to DNA methylation and ncRNAs could underlie the effects of fetal alcohol exposure in mice. *Dis Model Mech.* 2013; 6:977–92. <https://doi.org/10.1242/dmm.010975> PMID: 23580197
 24. Cruz FM, Tomé M, Bernal JA, Bernad A. miR-300 mediates Bmi1 function and regulates differentiation in primitive cardiac progenitors *Cell Death Dis.* 2015; 6:e1953. <https://doi.org/10.1038/cddis.2015.255> PMID: 26512961
 25. Shi X, Sun M, Liu H, Yao Y, Song Y. Long non-coding RNAs: a new frontier in the study of human diseases. *Cancer Lett.* 2013; 339:159–66. <https://doi.org/10.1016/j.canlet.2013.06.013> PMID: 23791884
 26. Boon RA, Hofmann P, Michalik KM, Lozano-Vidal N, Berghäuser D, Fischer A et al. Long Noncoding RNA Meg3 Controls Endothelial Cell Aging and Function: Implications for Regenerative Angiogenesis. *J Am Coll Cardiol.* 2016; 68:2589–91. <https://doi.org/10.1016/j.jacc.2016.09.949> PMID: 27931619
 27. Liu J, Li Q, Zhang KS, Hu B, Niu X, Zhou SM, et al. Downregulation of the Long Non-Coding RNA Meg3 Promotes Angiogenesis After Ischemic Brain Injury by Activating Notch Signaling. *Mol Neurobiol.* 2016; <https://doi.org/10.1007/s12035-016-0270-z>.
 28. Cui X, Jing X, Long C, Tian J, Zhu J. Long noncoding RNA MEG3, a potential novel biomarker to predict the clinical outcome of cancer patients: a meta-analysis. *Oncotarget.* 2017; 8:19049–56. <https://doi.org/10.18632/oncotarget.14987> PMID: 28157702
 29. Duan W, Du L, Jiang X, Wang R, Yan S, Xie Y et al. Identification of a serum circulating lncRNA panel for the diagnosis and recurrence prediction of bladder cancer. *Oncotarget* 2016; 7:78850–8. <https://doi.org/10.18632/oncotarget.12880> PMID: 27793008
 30. Zhang J, Liu SC, Luo XH, Tao GX, Guan M, Yuan H et al. Exosomal Long Noncoding RNAs are Differentially Expressed in the Cervicovaginal Lavage Samples of Cervical Cancer Patients. *J Clin Lab Anal.* 2016; 30:1116–21. <https://doi.org/10.1002/jcla.21990> PMID: 27184657
 31. Krueer TL, Dougherty SM, Reynolds L, Long E, de Silva T, Lockwood WW, et al. Expression of the lncRNA Maternally Expressed Gene 3 (MEG3) Contributes to the Control of Lung Cancer Cell Proliferation by the Rb Pathway. *PLoS One.* 2016; 11(11):e0166363. <https://doi.org/10.1371/journal.pone.0166363> PMID: 27832204
 32. Huang ZL, Chen RP, Zhou XT, Zhan HL, Hu MM, Liu B, et al. Long non-coding RNA MEG3 induces cell apoptosis in esophageal cancer through endoplasmic reticulum stress. *Oncol Rep.* 2017; 37:3093–9. <https://doi.org/10.3892/or.2017.5568> PMID: 28405686
 33. Xiu YL, Sun KX, Chen X, Chen S, Zhao Y, Guo QG, et al. Upregulation of the lncRNA Meg3 induces autophagy to inhibit tumorigenesis and progression of epithelial ovarian carcinoma by regulating activity of ATG3. *Oncotarget.* 2017; 8:31714–25. <https://doi.org/10.18632/oncotarget.15955> PMID: 28423647
 34. Gu L, Zhang J, Shi M, Zhan Q, Shen B, Peng C. lncRNA MEG3 had anti-cancer effects to suppress pancreatic cancer activity. *Biomed Pharmacother.* 2017; 89:1269–76. <https://doi.org/10.1016/j.biopha.2017.02.041> PMID: 28320094
 35. Fei C, Zhao Y, Guo J, Gu S, Li X, Chang C. Senescence of bone marrow mesenchymal stromal cells is accompanied by activation of p53/p21 pathway in myelodysplastic syndromes. *Eur J Haematol.* 2014; 93:476–86. <https://doi.org/10.1111/ejh.12385> PMID: 24889123
 36. Herman JG, Graff JR, Myöhänen S, Nelkin BD, Baylin SB, et al. Methylation-specific PCR: a novel PCR assay for methylation status of CpG islands. *Proc. Natl. Acad. Sci. USA* 1996; 93:9821–6. PMID: 8790415
 37. Kagami M et al. 2010. The IG-DMR and the MEG3-DMR at human chromosome 14q32.2: hierarchical interaction and distinct functional properties as imprinting control centers. *PLoS Genet.* 2010; 6: e1000992. <https://doi.org/10.1371/journal.pgen.1000992> PMID: 20585555
 38. Das PP, Hendrix DA, Apostolou E, Buchner AH, Canver MC, Beyaz S, et al. PRC2 Is Required to Maintain Expression of the Maternal Gtl2-Rian-Mirg Locus by Preventing De Novo DNA Methylation in Mouse Embryonic Stem Cells. *Cell Rep.* 2015; 12:1456–70. <https://doi.org/10.1016/j.celrep.2015.07.053> PMID: 26299972

39. Pino-Barrio MJ, García-García E, Menéndez P, Martínez-Serrano A. V-myc immortalizes human neural stem cells in the absence of pluripotency-associated traits. *PLoS One* 2015; 10 (3), e0118499. <https://doi.org/10.1371/journal.pone.0118499> PMID: 25764185
40. Villa A, Navarro-Galve B, Bueno C, Franco S, Blasco MA, Martínez-Serrano A. Long-term molecular and cellular stability of human neural stem cell lines. *Exp. Cell Res.* 2004; 294:559–70. <https://doi.org/10.1016/j.yexcr.2003.11.025> PMID: 15023542
41. Hackl M, Brunner S, Fortschegger K, Schreiner C, Micutkova L, Mück C, et al. miR-17, miR-19b, miR-20a, and miR-106a are down-regulated in human aging. *Aging Cell* 2010; 9:291–6. <https://doi.org/10.1111/j.1474-9726.2010.00549.x> PMID: 20089119
42. Chang TC, Wentzel EA, Kent OA, Ramachandran K, Mullendore M, Lee KH, et al. Transactivation of miR-34a by p53 broadly influences gene expression and promotes apoptosis. *Mol. Cell* 2007; 26: 745–52. <https://doi.org/10.1016/j.molcel.2007.05.010> PMID: 17540599
43. Raver-Shapira N, Marciano E, Meiri E, Spector Y, Rosenfeld N, Moskovits N, et al. Transcriptional activation of miR-34a contributes to p53-mediated apoptosis. *Mol. Cell* 2007; 26:731–43. <https://doi.org/10.1016/j.molcel.2007.05.017> PMID: 17540598
44. Lafferty-Whyte K, Cairney CJ, Jamieson NB, Oien KA, Keith WN. Pathway analysis of senescence-associated miRNA targets reveals common processes to different senescence induction mechanisms. *Biochim Biophys Acta* 2009; 1792:341–52. <https://doi.org/10.1016/j.bbadis.2009.02.003> PMID: 19419692
45. Park H, Park H, Pak HJ, Yang DY, Kim YH, Choi WJ, et al. miR-34a inhibits differentiation of human adipose tissue-derived stem cells by regulating cell cycle and senescence induction. *Differentiation* 2015; 90:91–100. <https://doi.org/10.1016/j.diff.2015.10.010> PMID: 26677981
46. Ogata T, Kagami M, Ferguson-Smith AC. Molecular mechanisms regulating phenotypic outcome in paternal and maternal uniparental disomy for chromosome 14. *Epigenetics* 2008; 3:181–7. PMID: 18698157
47. Lin SP, Youngson N, Takada S, Seitz H, Reik W, Paulsen M, et al. Asymmetric regulation of imprinting on the maternal and paternal chromosomes at the Dlk1-Gtl2 imprinted cluster on mouse chromosome 12. *Nat. Genet.* 2003; 35:97–102. <https://doi.org/10.1038/ng1233> PMID: 12937418
48. Stadtfeld M, Apostolou E, Ferrari F, Choi J, Walsh RM, Chen T, et al. Ascorbic acid prevents loss of Dlk1-Dio3 imprinting and facilitates generation of all-iPS cell mice from terminally differentiated B cells. *Nat. Genet.* 2012; 44:398–405. <https://doi.org/10.1038/ng.1110> PMID: 22387999
49. Xu X, Smorag L, Nakamura T, Kimura T, Dressel R, Fitzner A, et al. Dppa3 expression is critical for generation of fully reprogrammed iPS cells and maintenance of Dlk1-Dio3 imprinting. *Nat Commun.* 2015; 6:6008. <https://doi.org/10.1038/ncomms7008> PMID: 25613421
50. Luo Z, Lin C, Woodfin AR, Bartom ET, Gao X, Smith ER, Shilatifard A. Regulation of the imprinted Dlk1-Dio3 locus by allele-specific enhancer activity. *Genes Dev.* 2016; 30:92–101. <https://doi.org/10.1101/gad.270413.115> PMID: 26728555
51. Qian P, He XC, Paulson A, Li Z, Tao F, Perry JM, Guo F, et al. The Dlk1-Gtl2 Locus Preserves LT-HSC Function by Inhibiting the PI3K-mTOR Pathway to Restrict Mitochondrial Metabolism. *Cell Stem Cell* 2016; 18:214–28. <https://doi.org/10.1016/j.stem.2015.11.001> PMID: 26627594
52. Zhou Y, Zhang X, Klibanski A. MEG3 noncoding RNA: a tumor suppressor. *J. Mol. Endocrinol.* 2012; 8: R45–53.
53. Li X, Ao J, Wu J. Systematic identification and comparison of expressed profiles of lncRNAs and circRNAs with associated co-expression and ceRNA networks in mouse germline stem cells. *Oncotarget* 2017; 8:26573–90. <https://doi.org/10.18632/oncotarget.15719> PMID: 28404936
54. Lahbib-Mansais Y, Barasc H, Marti-Marimon M, Mompert F, Iannuccelli E, Robelin D, et al. Expressed alleles of imprinted IGF2, DLK1 and MEG3 colocalize in 3D-preserved nuclei of porcine fetal cells. *BMC Cell Biol.* 2016; 1; 17(1):35. <https://doi.org/10.1186/s12860-016-0113-9> PMID: 27716032
55. Yang Y, Wu J, Guan H, Cai J, Fang L, Li J, et al. MiR-136 promotes apoptosis of glioma cells by targeting AEG-1 and Bcl-2. *FEBS Lett.* 2012; 586:3608–12. <https://doi.org/10.1016/j.febslet.2012.08.003> PMID: 22967897
56. Tacutu R, Craig T, Budovsky A, Wuttke D, Lehmann G, Taranukha D, et al. Human Ageing Genomic Resources: integrated databases and tools for the biology and genetics of ageing. *Nucleic Acids Res.* 2013; 41(Database issue):D1027–33. <https://doi.org/10.1093/nar/gks1155> PMID: 23193293
57. Molina-Pinelo S, Salinas A, Moreno-Mata N, Ferrer I, Suarez R, Andrés-León E, et al. Impact of DLK1-DIO3 imprinted cluster hypomethylation in smoker patients with lung cancer. *Oncotarget* 2106; 10.18632/oncotarget.10611.
58. Brown WM. Exercise-associated DNA methylation change in skeletal muscle and the importance of imprinted genes: a bioinformatics meta-analysis. *Br J Sports Med.* 2015; 49:1567–78. <https://doi.org/10.1136/bjsports-2014-094073> PMID: 25824446

59. White RR, Milholland B, MacRae SL, Lin M, Zheng D, Vijg J, et al. Comprehensive transcriptional landscape of aging mouse liver. *BMC Genomics* 2015; 16:899. <https://doi.org/10.1186/s12864-015-2061-8> PMID: [26541291](https://pubmed.ncbi.nlm.nih.gov/26541291/)
60. Chandel NS, Jasper H, Ho TT, Passequé E. Metabolic regulation of stem cell function in tissue homeostasis and organismal ageing. *Nat Cell Biol.* 2016; 18:823–32. <https://doi.org/10.1038/ncb3385> PMID: [27428307](https://pubmed.ncbi.nlm.nih.gov/27428307/)